

Nanoengineered magnetic-field-induced superconductivity

Martin Lange,* Margriet J. Van Bael, Yvan Bruynseraede, and Victor V. Moshchalkov
 Laboratorium voor Vaste-Stoffysica en Magnetisme,
 K. U. Leuven, Celestijnenlaan 200D, 3001 Leuven, Belgium
 (Dated: May 21, 2019)

The perpendicular critical fields of a superconducting film have been strongly enhanced by using a nanoengineered lattice of magnetic dots (dipoles) on top of the film. Magnetic-field-induced superconductivity is observed in these hybrid superconductor / ferromagnet systems due to the compensation of the applied field between the dots by the stray field of the dipole array. By switching between different magnetic states of the nanoengineered field compensator, the critical parameters of the superconductor can be effectively controlled.

PACS numbers: 74.25.Dw 74.76.Db 75.75.+a

When the applied magnetic field exceeds a certain critical value, superconductivity is suppressed due to orbital and spin pair breaking effects. This very general property of superconductors sets strong limits for their practical applications, since, in addition to applied magnetic fields, the current sent through a superconductor also generates magnetic fields, which can lead to a loss of zero resistance. Materials that are not only able to withstand magnetic fields, but in which superconductivity can even be induced by applying a magnetic field, are very rare and up to now only $\text{Eu}_x\text{Sn}_{1-x}\text{Mo}_6\text{S}_8$ [1], and organic $\lambda\text{-(BETS)}_2\text{FeCl}_4$ materials [2, 3] show this unusual behavior. The appearance of magnetic-field-induced superconductivity (FIS) in these compounds was interpreted in terms of the Jaccarino-Peter effect [4], in which the exchange fields from the paramagnetic ions compensate an applied magnetic field, so that the destructive action of the field is neutralized.

Here we report that FIS can also be realized in hybrid superconductor / ferromagnet nanostructured bilayers. The basic idea of this nanoengineered FIS is quite straightforward (see Fig. 1). A lattice of magnetic dots is placed on top of a superconducting film, with the magnetic moments of all dots aligned along the positive z -direction. The field lines emanating from each dot are similar to those of a magnetic dipole, resulting in a positive value of the z -component of the magnetic induction B_z under the dots and in a negative value of B_z in the area between the dots, as shown in Fig. 1(a). Added to a homogeneous magnetic field H , see Fig. 1(b), these dipole fields *enhance* the z -component of the effective magnetic field $\mu_0 H_{\text{eff}} = \mu_0 H + B_z$ in the small area just *under the dots* and, at the expense of that, *reduce* H_{eff} *everywhere else* in the Pb film, thus providing the condition necessary for the FIS observation. This new field compensation effect is not restricted to specific superconductors, so that FIS could be achieved in any superconducting film in a certain magnetic field range mainly determined by the period of the dot array and the magnetic moment of each

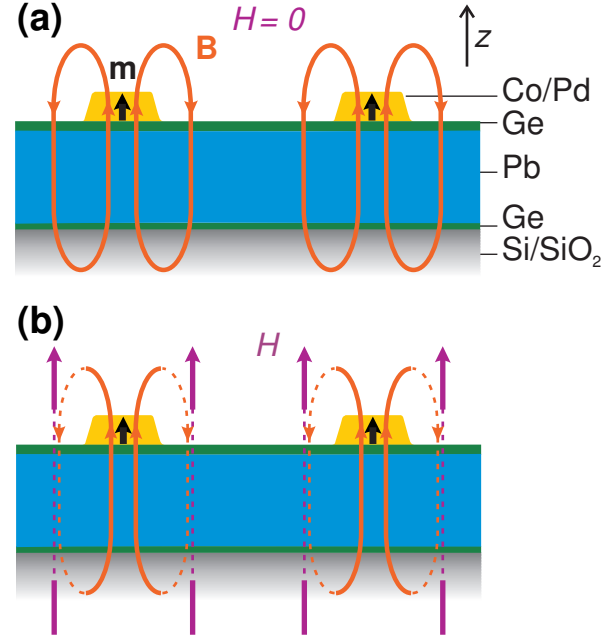


FIG. 1: Schematic drawing of the investigated hybrid superconductor / ferromagnet sample. (a) The magnetic moments m of the dots produce a magnetic stray field B that is comparable with the field of a magnetic dipole. (b) A magnetic field H applied in the z -direction can be compensated by the dipole stray field between the dots, resulting in the conditions necessary for the observation of magnetic field-induced superconductivity.

magnetic dot. This implies that the nanoengineered field compensator has the potential to enhance selectively the superconducting properties in high magnetic fields. To implement the idea of the nanoengineered FIS, we have prepared a sample, which reminds of other systems used during the last decade for studying flux pinning by periodic arrays of magnetic dots [5, 6, 7, 8, 9], magnetic antidots [10], and by magnetic domains [11]. The sample consists of a 85 nm superconducting Pb film evaporated on a 1 nm Ge base layer on an amorphous Si/SiO₂ substrate, which is held at liquid nitrogen temperature during deposition. This thin Pb-film behaves as a type-II

*Electronic address: martin.lange@fys.kuleuven.ac.be

superconductor. For protection against oxidation, the Pb is covered by a 10 nm Ge layer that is insulating at low temperatures and thus prevents the influence of the proximity effect between Pb and Co/Pd. The Ge/Pb/Ge tri-layer is patterned into a transport bridge (width 200 μm , distance between voltage contacts 630 μm) using optical lithography and chemical wet etching. The ferromagnetic dots are made by defining a resist mask on the transport bridge by electron-beam lithography and subsequent evaporation of a Pd(3.5 nm)/[Co(0.4 nm)/Pd(1.4 nm)]₁₀ multilayer into the resist mask. The resist is finally removed in a lift-off procedure. The dots are arranged in a regular square array with period 1.5 μm . They have a square shape (side length about 0.8 μm) with slightly irregular edges.

The dots on the superconducting Pb film consist of Co/Pd multilayers having an easy axis of magnetization perpendicular to the sample surface [12]. The hysteresis loop of the dots is measured with H perpendicular to the surface by magneto-optical Kerr effect, revealing a high magnetic remanance of $M_r = 0.8M_s$, where M_r and M_s are the remanent and saturation magnetization, respectively, and a large coercive field $\mu_0 H_{coe} = 150$ mT. This makes it possible to produce quite stable remanent magnetic domain states in the dots by using different magnetization procedures. These domain states were investigated by magnetic force microscopy (MFM) in a Digital Instruments nanoscope III. After demagnetization, the signal from each of the dots consists of dark and bright spots, as shown in Fig. 2(a), indicating the presence of several magnetic domains in the dots, compare Ref. [13]. The net magnetic moment m of each dot in this state is approximately zero ($m = |\mathbf{m}| = 0$). The demagnetization is carried out by oscillating H (perpendicular to the sample surface) around zero with decreasing amplitude. Saturating the dots in a large positive perpendicular field aligns all m along the positive z -direction ($m_z > 0$), so that the dots appear brighter compared with the signal between the dots, see Fig. 2(b). In contrast to that, when the dots have been saturated in a large negative field, resulting in $m_z < 0$, they give a darker contrast in the MFM image, as shown in Fig. 2(c). Simultaneous recording of magnetic and topographic images shows that the spots visible on dots in (b) and (c) are of topographic origin, and are not due to a magnetic signal.

The magnetic field (H)- temperature (T) - phase diagrams of the Pb film were constructed for the three magnetic states of the dots from $\rho(T)$ -measurements carried out in a Quantum Design Physical Properties Measurement System applying a 4-probe ac technique with an ac-current of 10 μA at a frequency of 19 Hz. H is applied perpendicular to the sample surface. We defined the critical temperature as $T_c = T(\rho = 50\%\rho_n)$, with ρ the resistivity and $\rho_n = 1.4 \mu\Omega \text{ cm}$ the normal state resistivity at 7.3 K. We did not observe any indication that the small magnetic fields $|H| \ll H_{coe}$ applied during these measurements altered the domain state of the dots, although minor microscopic changes cannot be ex-

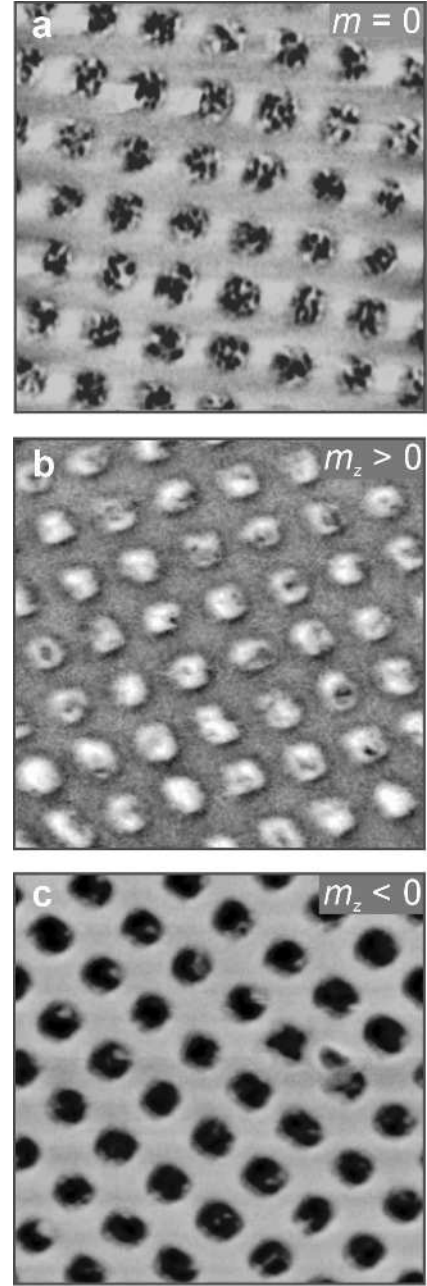


FIG. 2: MFM images of the hybrid superconductor / ferromagnet structure in $H = 0$ and at room temperature. The images show a $10 \times 10 \mu\text{m}^2$ region of the sample in the remanent state after (a) demagnetization, (b) magnetization in $H = +1$ T, (c) magnetization in $H = -1$ T.

cluded.

The H - T -phase boundary separating the normal (N) from the superconducting (S) state is clearly altered by changing the magnetic state of the dot array. A conventional symmetric (with respect to H) phase boundary is obtained when $m = 0$, see Fig. 3(a). Two kinks in the curve can be seen at $H = \pm H_1$, with H_1 the first matching field $\mu_0 H_1 = \phi_0 / (1.5 \mu\text{m})^2 = 0.92$ mT, at which

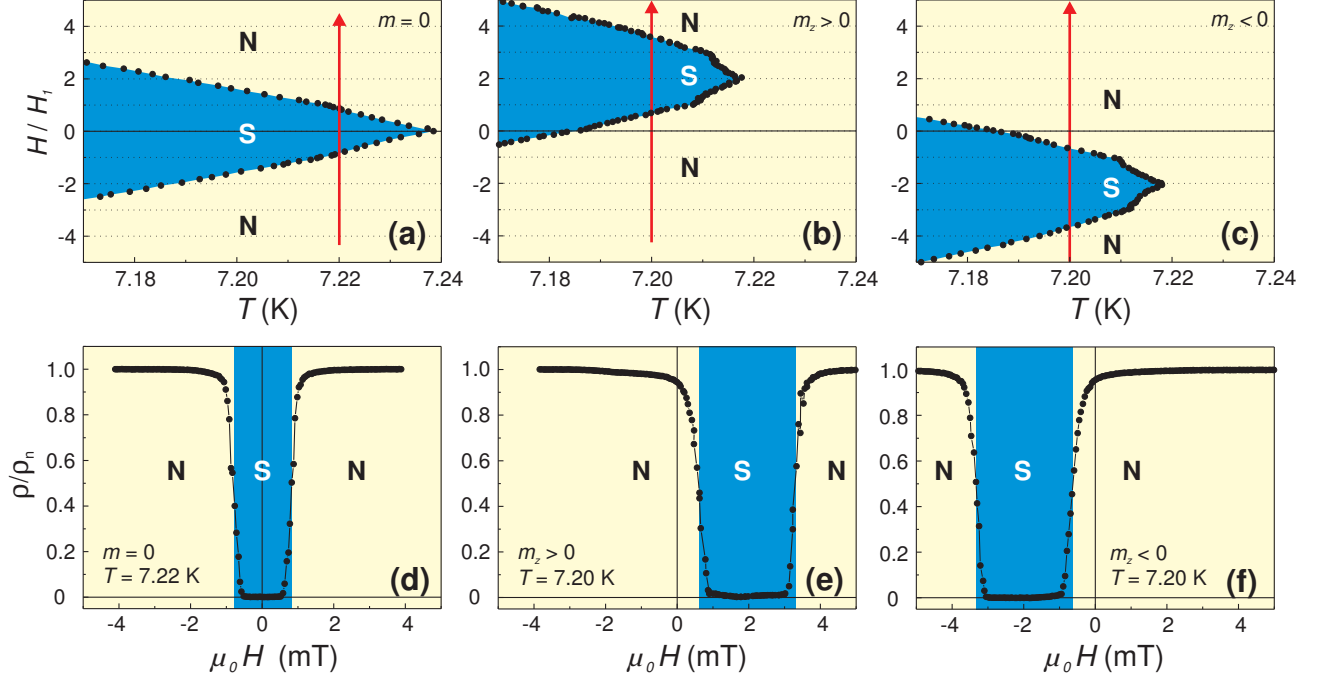


FIG. 3: Field - induced superconductivity (FIS) in a Pb film with an array of magnetic dots. Blue and yellow areas correspond to the superconducting (S) and the normal state (N), respectively. The H - T -phase diagrams are obtained after (a) demagnetization ($m = 0$), (b) saturation of the dots in a large positive H ($m_z > 0$), (c) saturation in a large negative H ($m_z < 0$). $\rho(H)$ is shown for the magnetic states (d) $m = 0$, (e) $m_z > 0$, and (f) $m_z < 0$, measured at lines of constant T as indicated by red arrows in the corresponding phase diagrams.

the applied flux per unit cell of the dot array is exactly one superconducting flux quantum $\phi_0 = 2.07 \text{ mT } \mu\text{m}^2$. In contrast to that, the H - T -phase boundary is strongly asymmetric with respect to H when the dots are magnetized in positive or negative directions, see Figs. 3(b) and 3(c). Moreover, the maximum T_c is shifted to $+2H_1$ when $m_z > 0$ and to $-2H_1$ when $m_z < 0$. This shift gives rise to FIS when $m_z > 0$ and $m_z < 0$, as is demonstrated in Figs. 3(e) and 3(f). For instance, for $m_z > 0$ and $T = 7.20 \text{ K}$, the sample is in the normal state in zero field, but when a positive field between $+0.6 \text{ mT}$ and $+3.3 \text{ mT}$ is applied, the Pb film becomes superconducting, as shown in Fig. 3(e). Similarly, when the magnetic state of the dots is switched to $m_z < 0$, superconductivity is induced by applying a negative field between -3.3 mT and -0.6 mT , see Fig. 3(f). Contrary to that, the $\rho(H)$ curve shows the typical NSN transition of a conventional superconductor for $m = 0$.

In the present system, the FIS can be explained by taking into account the local magnetic induction of the dots \mathbf{B} , as was already qualitatively shown in the discussion of Fig. 1. To support further these arguments, we give in Fig. 4(a) the distribution of B_z , the z -component of \mathbf{B} for $m_z > 0$ in the x - y -plane, calculated by using a magnetostatic model (see, e.g., Ref. [14]). In zero field (Fig. 4(a)) the magnetic dipoles generate stray fields exceeding the upper critical field of the Pb film when $T > 7.185 \text{ K}$, and, as a result, the Pb film is in the normal state. In an

applied field of $H = +H_2$, the compensation of B_z takes place in the interdot area where the Pb film is now in the superconducting state (see the blue color in Fig. 4(b)), thus providing the percolation through dominantly superconducting areas, and making possible the continuous flow of Cooper pairs and zero film resistance.

An important feature to note here is the appearance of periodic kinks in the H - T -phase boundary with a period coinciding with the first matching field H_1 . These kinks are due to fluxoid quantization effects [15], confirming that superconductivity indeed nucleates in multiply connected regions of the film, like in superconducting wire networks [16] or thin films with periodic arrays of antidots [17, 18]. The maximum T_c at exactly $H = +2H_1$ can therefore be understood in terms of fluxoid quantization: the flux created by the stray field between the dots can be estimated from the magnetostatical calculations to be about $-2.1\phi_0$ per unit cell of the dot array. This makes $H = +2H_1$ a favorable field for fulfilling the fluxoid quantization constraint. Similar arguments can also be applied for the dots in the $m_z < 0$ state to explain the shift of the maximum T_c to $H = -2H_1$. For $m = 0$, \mathbf{B} is strongly reduced due to the domain structure in the dots. This means that the stray field only weakly influences the Pb film, leading to a phase boundary without peculiarities except the weak kinks at $H = \pm H_1$. To understand all features in the phase boundaries in more details, one should solve the linearized Ginzburg-Landau (GL) equa-

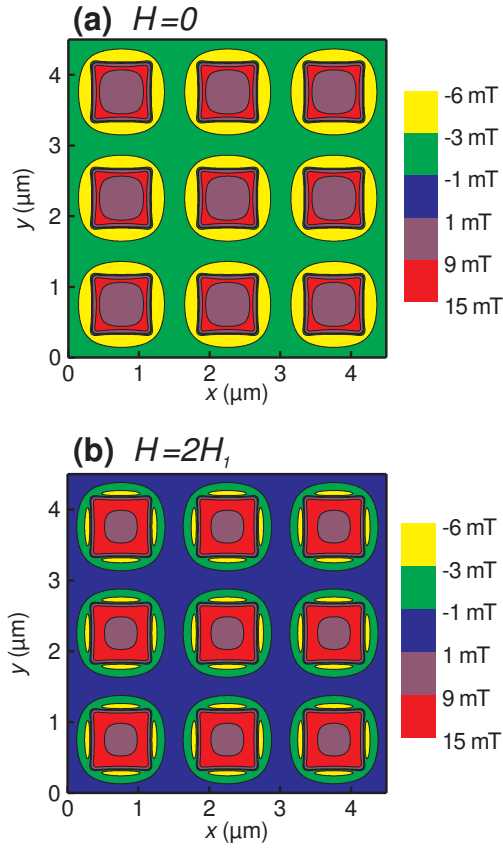


FIG. 4: Contour plots of the z -component of the effective magnetic field $\mu_0 H_{eff} = \mu_0 H + B_z$ in the superconductor, calculated using a magnetostatic model, for (a) $H = 0$, (b) for $H = +2H_1$.

tions, taking explicitly into account the additional vector

potential created by the magnetic dots. This work has not been done yet, but the GL analysis of the flux distribution around magnetic dots has been already reported in Ref. [19].

The field region in which FIS is observed can be tuned by changing the parameters of the nanoengineered field compensator, such as the period of the dot array or the magnitude of the stray field. For instance, an increase of the fields emanating from the dots could be achieved by using magnetic dipoles with larger magnetic moments, shifting the maximum of T_c to an even higher applied field. Good candidates for that are arrays of nanodots [20] and nanopillars [21], where the out-of-plane magnetization occurs due to shape anisotropy. Using focused ion beam lithography [22], dot arrays with a period of 70 nm have been fabricated, corresponding to a first matching field of $H_1 \approx 0.4$ T, which is already a remarkably high field. Besides improving the critical fields, the dipole array field compensator can also be used to design logical devices in which superconductivity is controlled by switching between the two polarities of the magnetized dot array.

In conclusion, we have shown that a nanoengineered lattice of magnetic dipoles can be used to selectively enhance the critical fields of superconducting films. Magnetic-field-induced superconductivity is observed due to the compensation of the applied field by the stray field of the dipoles.

The authors are thankful to E. Claessens for help with the measurements, and to S. Raedts, M. Morelle and K. Temst for their contribution to the sample preparation. This work was supported by the Belgian IUAP and the Flemish GOA programs, by the ESF "VORTEX" program, and by the Fund for Scientific Research (F.W.O.) - Flanders. M.J.V.B. is a Postdoctoral Research Fellow of the F.W.O.-Flanders.

-
- [1] H. W. Meul et al., Phys. Rev. Lett. **53**, 497 (1984).
 - [2] S. Uji et al., Nature **410**, 908 (2001).
 - [3] L. Balicas et al., Phys. Rev. Lett. **87**, 067002 (2001).
 - [4] V. Jaccarino and M. Peter, Phys. Rev. Lett. **9**, 290 (1962).
 - [5] O. Geoffroy et al., J. Magn. Magn. Mater. **121**, 223 (1993).
 - [6] J. I. Martín et al., Phys. Rev. Lett. **79**, 1929 (1997).
 - [7] D. J. Morgan and J. B. Ketterson, Phys. Rev. Lett. **80**, 3614 (1998).
 - [8] M. J. Van Bael et al., Phys. Rev. B **59**, 14674 (1999).
 - [9] M. J. Van Bael et al., Physica C **332**, 12 (2000).
 - [10] M. Lange et al., Europhys. Lett. **53**, 646 (2001); **56**, 149 (2002).
 - [11] M. Lange et al., Appl. Phys. Lett. **81**, 322 (2002).
 - [12] P. F. Carcia, A. D. Meinhaldt, and A. Suna, Appl. Phys. Lett. **47**, 178 (1985).
 - [13] M. Hehn et al., Science **272**, 1782 (1996).
 - [14] J. D. Jackson, *Classical Electrodynamics* (Wiley, New York, ed. 3, 1999).
 - [15] W. A. Little and R. D. Parks, Phys. Rev. Lett. **9**, 9 (1962).
 - [16] V. V. Moshchalkov et al., in *Quantum Coherence in Mesoscopic Systems*, edited by B. Kramer (Plenum Press, New York, 1991), p. 457.
 - [17] A. Bezryadin and B. Pannetier, J. Low. Temp. Phys. **98**, 251 (1995).
 - [18] V. V. Moshchalkov et al., in *Handbook of Nanostructured Materials and Nanotechnology*, edited by H. S. Nalwa (Academic Press, San Diego, 2000), vol. 3, chap. 9, p. 451.
 - [19] M. V. Milosevic, S. V. Yampolskii, and F. M. Peeters, Phys. Rev. B **66**, 024515 (2002).
 - [20] C. A. Ross et al., J. Appl. Phys. **91**, 6848 (2002).
 - [21] S. Y. Chou et al., J. Appl. Phys. **76**, 6673 (1994).
 - [22] K. Koike et al., Appl. Phys. Lett. **78**, 784 (2001).